https://doi.org/10.1590/jatm.v18.1444 ORIGINAL PAPER

Comparative Study of Linear Regression Models for the Infrared Reflection Spectroscopic Determination of Magnesium, Teflon, and Viton Pyrotechnic Compositions

Bruno Henrique Santos Julio[1,2,*], Jennifer Alves Cavalcante[1], Milton Faria Diniz[2], Rita de Cássia Lazzarini Dutra[1]

1. Departamento de Ciência e Tecnologia Aeroespacial – Instituto Tecnológico de Aeronáutica – Divisão de Ciências Fundamentais – São José dos Campos/SP – Brazil.
2. Departamento de Ciência e Tecnologia Aeroespacial – Instituto de Aeronáutica e Espaço – Divisão de Propulsão – São José dos Campos/SP – Brazil.

***Corresponding author:** juliobhsj@fab.mil.br

ABSTRACT

The pyrotechnic composition of magnesium, Teflon, and Viton (MTV) is employed in solid rocket motor initiation systems, flares, and other applications. No studies addressing its quantification or evaluating statistical models have been reported in the consulted and available literature. Infrared spectroscopy enables the quantification of each component of a system in a fast and non-destructive manner. This study presents the application of the universal attenuated total reflection technique to the analysis of five laboratory-prepared samples with different MTV contents, in which the analytical bands of each component were used in calibration curves through different linear regression models. The test sample results demonstrate adequate agreement between the methodologies, with relative errors below 6.5% for the quantification of Viton and Teflon, with the estimation of Teflon being improved by the use of weighted linear regression. For magnesium, both the simple and weighted regression estimates fall outside the 95% confidence interval, indicating the presence of systematic error. The contribution to the state of the art lies in the evaluation of MTV (as-received samples) through infrared reflection techniques, using different statistical treatments, including those specifically designed for spectroscopic data.

Keywords: Infrared spectroscopy; Pyrotechnic; Magnesium Teflon Viton; Regression analysis.

INTRODUCTION

In a solid rocket motor, the igniter is the component responsible for initiating the combustion of the propellant grain. When activated, it produces a flame that provides sufficient energy to simultaneously ignite the entire internal surface of the grain. Pelletized and pyrogen igniters are employed in Brazilian rockets, the latter also being initiated by a basket of pellets (Palmerio 2017).

Pyrotechnic compositions used in igniter pellets are mixtures of materials capable of self-sustained combustion when properly initiated, producing a specific effect. The basis of any pyrotechnic formulation consists of an oxidizer and a fuel, together with a binder to provide mechanical properties (Agrawal 2010).

Received: Feb. 27, 2026 | **Accepted:** Apr. 10, 2026
Peer Review History: Single Blind Peer Review.
Section editor: Cristina Andrade

The mechanical properties associated with the pellets are directly related to the polymer selected for the pyrotechnic mixture, and its compatibility with the fuel and oxidizer must be assessed in order to improve stability and, consequently, ensure an adequate service life of the product. Examples of binders include polyester, Viton (a fluoropolymer of hexafluoropropylene and vinylidene fluoride), and polyol-based resins (Dozono 2003).

Magnesium, Teflon, and Viton (MTV) compositions are used in the space sector for rocket motor ignition systems, in granular form and as small pellets, such as those employed in the satellite launch vehicle (Barros 2016).

Koch (2002) presents a ternary diagram representing the applications of the MTV composition as a function of the mass fraction (ω) of each of its components. According to this study, the proportion of each component can be adjusted within established ranges to meet the requirements of different applications. This highlights the importance of quantitative knowledge of the MTV pyrotechnic composition, as it is directly correlated with the performance and suitability of the mixture for specific uses.

According to Thompson (2018), quantitative methodologies based on Fourier-transform infrared spectroscopy (FT-IR) rely on the Beer-Lambert law, according to which absorbance varies linearly with the concentration of the material component. Quantitative analysis performs best in the absence of band overlap and can be employed to examine multicomponent systems.

The characterization of MTV has been addressed in several studies, such as the accelerated aging of flares conducted by Pires *et al.* (2017) and the investigation of the effect of hygrothermal aging on MTV decomposition reactions by Gaunekar and Ambekar (2024), both providing qualitative and structural information about these materials. However, in the consulted and available literature, no references describing quantitative methodologies for determining the components were found.

In the present work, the use of FT-IR with universal attenuated total reflection (UATR) is proposed for the quantification of the components in an MTV pyrotechnic composition. This technique is rapid, requires minimal or no sample preparation, and can be applied to a variety of sample types (Thompson 2018). Errors associated with the reflection technique can be significant if mathematical resources are not employed in certain cases – for example, the use of relative bands (in practice, dividing the absorbance values of two bands from the same spectrum) to minimize variations in analytical band intensity due to changes in optical path length. This study compares the results obtained for a test sample using analytical bands – that is, without mathematical adjustment – through calibration curves generated by simple linear regression, weighted linear regression, and linear regression with confidence intervals (CIs), to evaluate the performance of each methodology.

METHODOLOGY

Materials and equipment

The materials used in the MTV pyrotechnic compositions were magnesium from Merck KGaA, in the form of particles smaller than 1 mm; Teflon, from DuPont, with a particle size range between 35 mesh and 150 mesh; Viton, also from DuPont, as a binder in flake form; and P.A. acetone from Synth, used as a solvent. The following equipment was used: a SHIMADZU analytical balance, model ATY 224; a FANEM oven, model 320-SE; and a Perkin Elmer FT-IR spectrometer with a UATR accessory, model Frontier.

Preparation of MTV compositions

The MTV samples were produced at the Laboratório de Pirotecnia of the Instituto de Aeronáutica e Espaço (IAE), with a total mass of 5 g each, and coded as A1 to A5. The manufacturing process of the MTV samples employed the proportions presented in Table 1. Initially, the components were weighed on an analytical balance. Next, Viton was dissolved in acetone in a glass container. After complete dissolution, Teflon and magnesium powder were added, and the mixture was manually homogenized until the solvent completely evaporated. The resulting mixture was then dried in an oven at 60 °C for approximately 2 hours. Subsequently, an additional test sample, designated A_{test}, was prepared following the same methodology.

Table 1. Sample preparation formulations.

Sample	Compositions percentages		
	Magnesium	Teflon	Viton
A1	34	62	4
A2	40	51	9
A3	46	40	14
A4	51	30	19
A5	56	20	24
Atest	25	60	15

Source: Elaborated by the authors.

FT-IR/UATR analysis

The FT-IR/UATR analysis was performed at the Laboratório de Análise Instrumental of IAE. The samples A1 to A5 were manually ground in an agate mortar to improve homogenization of the pyrotechnic mixture. Each sample was then subjected to five independent measurements of the analytical band height using the spectrometer in the medium infrared region (mid-IR) (4,000-550 cm^{-1}), with a resolution of 4 cm^{-1}, 20 scans, and an 80 N force applied to the samples. Baselines used to determine the heights of the analytical bands are described in the Results and Discussion section.

Figure 1 shows a flowchart illustrating the experimental sequence for obtaining the FT-IR calibration curves.

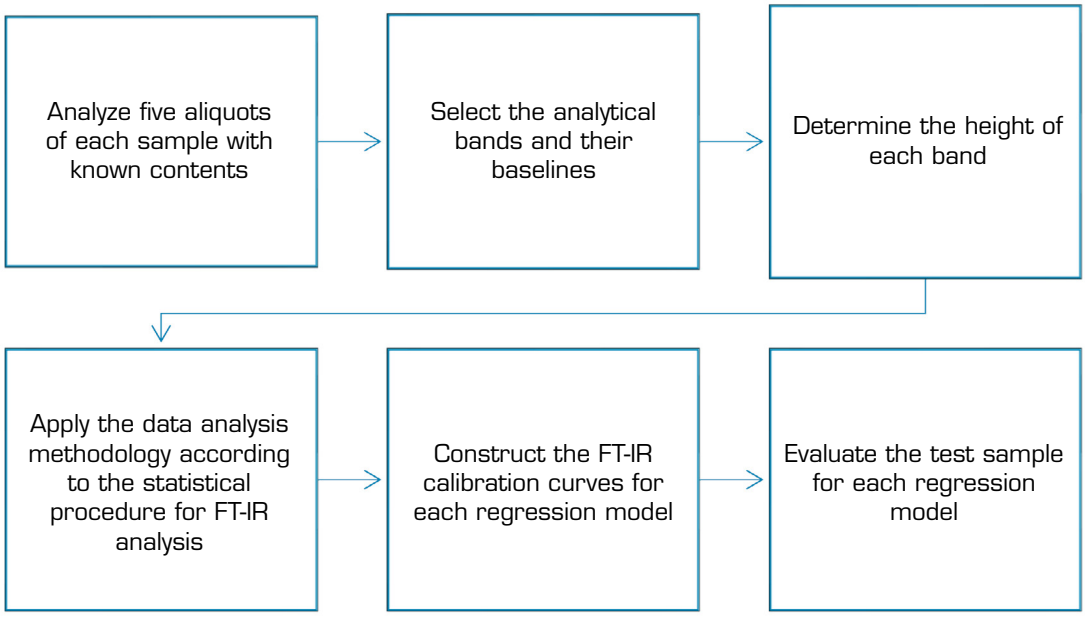

Source: Adapted from Dutra and Soares (1998); Dutra *et al.* (1996); Horák and Vítek (1978); Smith (1979).

Figure 1. Quantitative FT-IR/UATR analysis flowchart.

Data analysis

The system of equations established by Horák and Vítek (1978), with a specific statistical treatment for infrared analysis, is applied when a limited number of experimental values is available. In this approach, the median value ($\hat{\mu}$), rather than the arithmetic mean, is used to minimize the influence of outlying values.

The standard deviation ($\hat{\sigma}$) is obtained using Eq. 1, where R is the difference between the highest and lowest reflectance values ($x_n - x_1$) and K_R is the coefficient for standard deviation calculation (for five values, $K_R = 0.430$):

$$\hat{\sigma} = K_R . R \tag{1}$$

The median standard deviation ($\hat{\sigma}_{\hat{\mu}}$) can be calculated using Eq. 2, where n is the number of measurements:

$$\hat{\sigma}_{\hat{\mu}} = \frac{\hat{\sigma}}{\sqrt{n}} \tag{2}$$

The relative deviation for each sample is calculated according to Eq. 3. The methodological error can be defined as the median of the relative errors (Dutra and Soares 1998; Dutra *et al.* 1996):

$$RD\ (\%) = \left(\frac{\hat{\sigma}_{\hat{\mu}}}{\hat{\mu}}\right) . 100 \tag{3}$$

Simple linear regression

In simple linear regression, it is assumed that errors occur only in the y variable, while the x values (standard concentrations) are considered exact. The objective is to determine the line that minimizes the differences in the y direction between the experimental data points and the fitted line (Miller and Miller 2010). The slope (b) and intercept (a) coefficients are calculated using Eqs. 4 and 5, respectively:

$$b = \frac{\sum_i [(x_i - \bar{x})(y_i - \bar{y})]}{\sum_i (x_i - \bar{x})^2} \tag{4}$$

$$a = \bar{y} - b\bar{x} \tag{5}$$

where: $\bar{x}$ *e* $\bar{y}$ is centroid of the data points and x_i and y_i: are the experimental values.

Weighted linear regression

If the regression errors have constant variance (homoscedasticity), simple linear regression is appropriate; otherwise, in the presence of heteroscedasticity, it loses efficiency and introduces errors, suggesting the use of weighted regression (Farias *et al.* 2015; Miller and Miller 2010).

According to Farias *et al.* (2015), weighted linear regression employs the coefficients of the analytical curve so as to assign greater weight to points where error bars are smaller; in other words, it is more important for the fitted line to pass closer to the points with lower error. The individual weights (w_i) can be calculated using Eq. 6 (Farias *et al.* 2015; Miller and Miller 2010):

$$w_i = \frac{s_i^{-2}}{\sum_i s_i^{-2}/n} \tag{6}$$

where n: is the number of samples and s_i^2 is the sample variance.

The slope (b_w) and intercept (a_w)coefficients are calculated using Eqs. 7 and 8, respectively:

$$b_w = \frac{\sum_i w_i x_i y_i - n\bar{x}_w \bar{y}_w}{\sum_i w_i x_i^2 - n\bar{x}_w^2} \tag{7}$$

$$a_w = \bar{y}_w - b_w \bar{x}_w \tag{8}$$

where $\bar{y}_w = \Sigma_i w_i y_i / n$: is the y-coordinate of the weighted centroid and $\bar{x}_w = \Sigma_i w_i x_i / n$: is the x-coordinate of the weighted centroid.

Simple linear regression with CI

The predictions obtained from simple linear regression generally deviate from the experimental observations. To evaluate this discrepancy in estimating the concentration value (x_0) from a measured experimental response (y_0), the standard deviation of the concentration associated with the regression (S_{x0}) is considered, as defined in Eqs. 9 and 10 (Farias *et al.* 2015; Miller and Miller 2010):

$$S_{y/x} = \sqrt{\frac{\sum_i (y_i - \hat{y}_i)^2}{(n-2)}} \tag{9}$$

$$S_{x_0} = \frac{S_{y/x}}{b}\sqrt{\frac{1}{m} + \frac{1}{n} + \frac{(y_0 - \bar{y})^2}{b^2 \sum_i (x_i - \bar{x})^2}} \tag{10}$$

where $S_{y/x}$: is the standard deviation of the regression along the y axis, b: is the slope of the regression line, y_0: is the median experimental value of the test sample, $\hat{y}_i$: values is the value predicted by the regression, x_i and y_i: are the experimental values, m: is the number of measurements used to determine x_0; , and n: is the number of samples.

Equation 11 is used to determine the CI for x_0. For this purpose, the t-Student value corresponding to the desired confidence level and (n – 2) degrees of freedom is employed, to account for the uncertainty associated with the estimate:

$$CI = x_0 \pm t_{(n-2)} S_{x_0} \tag{11}$$

Coefficient of determination

According to Miller and Miller (2010), in the case of simple linear regression, the coefficient of determination (R^2) can be calculated using Eq. 12, based on the previously defined parameters:

$$R^2 = 1 - \frac{\sum_i (y_i - \hat{y}_i)^2}{\sum_i (y_i - \bar{y})^2} \tag{12}$$

For weighted linear regression, Eq. 12 is modified to include the individual weights (w_i) in the calculation of the weighted coefficient of determination (R_w^2), resulting in Eq. 13. However, the coefficients R^2 and R_w^2 are not directly comparable, as they reflect different approaches to handling the variability of the response variable (Draper and Smith 1998):

$$R_w^2 = 1 - \frac{\sum_i w_i (y_i - \hat{y}_i)^2}{\sum_i w_i (y_i - \bar{y}_w)^2} \tag{13}$$

RESULTS AND DISCUSSION

Selection of analytical bands

The selection of analytical bands, i.e., those associated with the component to be determined, was based on the increase or decrease in band intensity according to the corresponding variation in component content, in accordance with the Beer-Lambert law, and on the absence of band overlap (Smith 1979).

In Fig. 2, the analytical bands of each component are presented, as well as the region of band overlap, highlighted for better visualization, facilitating the understanding of why bands within this range were not selected. Although magnesium does not produce characteristic infrared bands due to its metallic nature, it is detected through a weak absorption at 3,694 cm^{-1}, assigned to the νO-H stretching, caused by $Mg(OH)_2$ formation. This was selected as a parameter indirectly related to magnesium (FT-IR spectrum) (Fig. 2a) (Gaunekar and Ambekar 2024; Zahir *et al.* 2019). For Teflon (FT-IR spectrum) (Fig. 2b), the strong band at 1,201-1,147 cm^{-1}, corresponding to the νC-F_2 stretching, was not selected due to overlap with the Viton band at 1,190 cm^{-1}; instead, the band at 637 cm^{-1}, corresponding to the δC-F_2 bending, was chosen (Koch 2012). For Viton (FT-IR spectrum)(Fig. 2c), the analytical band at 1,397 cm^{-1}, corresponding to the νC-F_3 stretching, was used, being outside the overlap region with Teflon bands (Mattos *et al.* 2009). The aforementioned characteristic bands are highlighted in the MTV composition (FT-IR spectrum) (Fig. 2d).

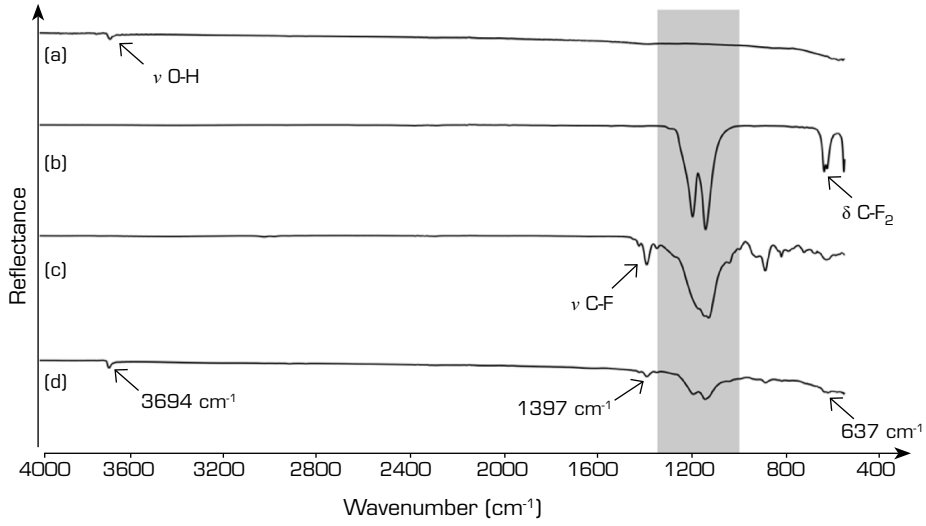

Source: Elaborated by the authors.

Figure 2. FT-IR/UATR spectra of the as-received sample, highlighting the characteristic analytical bands assigned to: (a) Magnesium; (b) Teflon; (c) Viton; and (d) MTV.

Tables 2–4 present the FT-IR/UATR data obtained from the heights of the analytical bands corresponding to magnesium, Teflon, and Viton, respectively, as illustrated in Fig. 2.The median values of the analytical bands increase or decrease according to the content of the components, according to the Lambert-Beer law (Smith 1979). The baselines for obtaining the heights of the analytical bands at 3,694, 637, and 1,397 cm^{-1} were established within the wavenumber ranges of 3,720-3,660 cm^{-1}, 668-597 cm^{-1}, and 1,570-1,333 cm^{-1}, respectively. Methodological errors ranged from 7% to 11%, which were considered satisfactory under the analysis conditions: reflection mode (Barros *et al.* 2025), as-received samples, and measurement of medium to low-intensity bands. For the regression calculations, the percentage concentrations were normalized to the 0-1 range.

Table 2. FT-IR/UATR data for samples A1 to A5: A_{3694} versus magnesium content.

Sample	Magnesium (%)	A_{3694} Median value	Standard deviation of the median ($\hat{\sigma}_{\tilde{\mu}}$)	Relative error (%)	Error of the method (%)
A1	34	0.014	0.001	7	
A2	40	0.018	0.002	11	
A3	46	0.024	0.004	17	11
A4	51	0.028	0.003	11	
A5	56	0.032	0.003	9	

Source: Elaborated by the authors.

Table 3 .FT-IR/UATR data for samples A1 to A5: A_{637} versus Teflon content.

Sample	Teflon (%)	A_{637} Median value	Standard deviation of the median ($\hat{\sigma}_{\hat{\mu}}$)	Relative error (%)	Error of the method (%)
A1	62	0.127	0.002	2	
A2	51	0.100	0.010	10	
A3	40	0.097	0.013	13	10
A4	30	0.035	0.011	31	
A5	20	0.029	0.003	10	

Source: Elaborated by the authors.

Table 4. FT-IR/UATR data for samples A1 to A5: A_{1397} versus Viton content.

Sample	Viton (%)	A_{1397} Median value	Standard deviation of the median ($\hat{\sigma}_{\hat{\mu}}$)	Relative error (%)	Error of the method (%)
A1	4	0.011	0.001	9	
A2	9	0.015	0.001	7	
A3	14	0.025	0.001	4	7
A4	19	0.026	0.002	8	
A5	24	0.041	0.002	5	

Source: Elaborated by the authors.

In Table 5, only the FT-IR/UATR data corresponding to the test sample are included. The discussion of the data was carried out after the construction of the calibration curves.

Table 5. FT-IR/UATR data for the as-received test sample: $A_{3694,}$ $A_{637\ e}$ A_{1397}.

A_{3694}	Parameters	A_{637}	Parameters	A_{1397}	Parameters
0.014	$\hat{\mu}$ = 0.014	0.116	$\hat{\mu}$ = 0.116	0.029	$\hat{\mu}$ = 0.025
0.020	R = 0.009	0.078	R = 0.057	0.031	R = 0.006
0.011	$\hat{\sigma}$ = 0 0.004	0.128	$\hat{\sigma}$ = 0.025	0.025	$\hat{\sigma}$ = 0.003
0.018	$\hat{\sigma}_{\hat{\mu}}$ = 0.002	0.073	$\hat{\sigma}_{\hat{\mu}}$ = 0.011	0.025	$\hat{\sigma}_{\hat{\mu}}$ = 0.001
0.013	RD = 14 %	0.130	RD = 9 %	0.025	RD = 4%

Source: Elaborated by the authors.

Simple linear regression

In Fig. 3, the simple linear regression for quantifying magnesium content, A_{3694} versus magnesium content (Eq. 14), is presented, with a coefficient of determination (R^2) of 0.997, obtained from the data in Table 2.

$$A_{3694} = 0.0836[magnesium] - 0.0148 \quad (14)$$

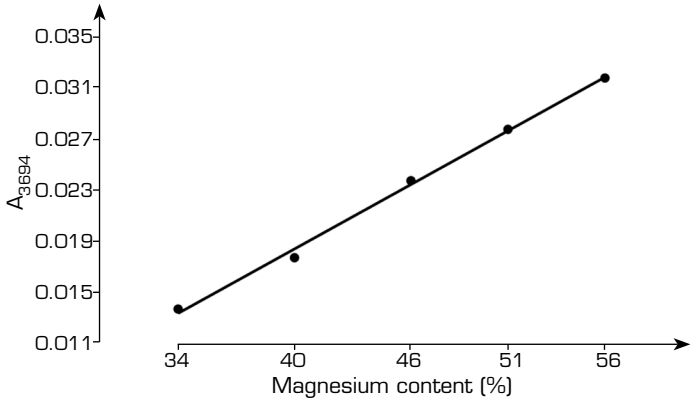

Source: Elaborated by the authors.

Figure 3. Simple linear regression for magnesium quantification.

For the determination of Teflon content, the simple linear regression of A_{637} versus Teflon content (Eq. 15), with $R^2 = 0.902$ is shown in Fig. 4, based on the data in Table 3.

$$A_{637} = 0.2476[Teflon] - 0.0229 \quad (15)$$

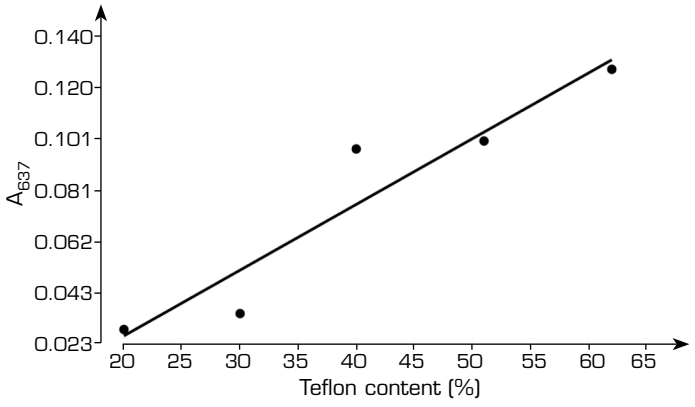

Source: Elaborated by the authors.

Figure 4. Simple linear regression for Teflon quantification.

In Fig. 5, Viton content was assessed using the simple linear regression of A_{1397} versus Viton content (Eq. 16), with $R^2 = 0.928$, obtained from the data in Table 4.

$$A_{1397} = 0.1420[Viton] + 0.0037 \quad (16)$$

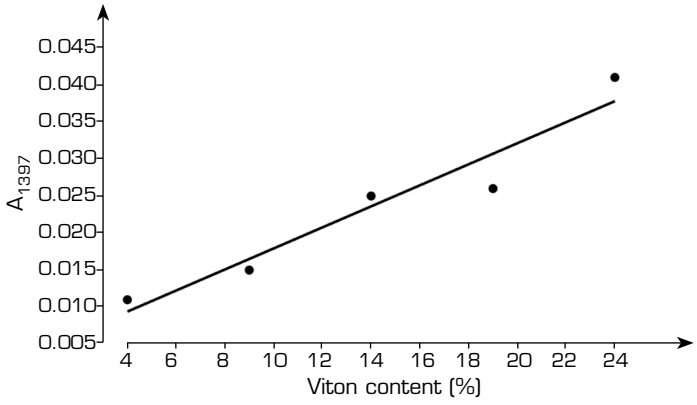

Source: Elaborated by the authors.

Figure 5. Simple linear regression for Viton quantification.

The median values of the test sample (Table 5) were applied to the system of Eqs. 14–16, yielding the results presented in Table 6.

Table 6. Test sample results obtained by simple linear regression.

Component	Nominal content (%)	Simple linear regression	Determined content (%)	Absolute deviation (%)
Magnesium	25	Eq. 14	34.4	+9.4
Teflon	60	Eq. 15	56.1	-3.9
Viton	15	Eq. 16	15.0	0.0

Source: Elaborated by the authors.

Analysis of Table 6 shows that the magnesium content estimated using Eq. 14 exhibited limited accuracy, with an absolute deviation of +9.4%, despite a high coefficient of determination ($R^2 = 0.997$). The calibration points (Table 2) showed relative errors of 7-17%, likely due to the low intensity of the selected analytical band (A_{3694}), while the test sample had a relative error of 14% (Table 5). For Teflon, the estimated content of 56.1% obtained from Eq. 15 closely matched the reference value, although the fit $R^2 = 0.902$ suggests potential for model refinement. Relative errors for the calibration points ranged from 2% to 31% (Table 3), with 9% for the test sample (Table 5). In the case of Viton, smaller relative errors were observed, ranging from 4% to 9% for the calibration points (Table 4) and 4% for the test sample (Table 5). Consequently, Eq. 16 provided an accurate estimation of the expected content (15%), with the model showing a coefficient of determination of $R^2 = 0.928$, indicating a satisfactory fit.

Weighted linear regression

Although residual analysis did not indicate heteroscedasticity, weighted linear regression was employed. This approach is recommended when the variances of the observations differ, as weighted least squares produce more accurate estimates than ordinary least squares (Montgomery *et al.* 2012). The choice is justified by the significant variation in the relative errors of the analytical band heights, which ranged from 2% to 31%, allowing more precise observations to carry greater weight in the model fit.

Figure 6 presents the weighted linear regression for the quantification of magnesium content, A_{3694} versus magnesium content (Eq. 17), with $R_w^2 = 0.996$, obtained from the data in Table 2. The vertical bars indicate the variance observed for each sample.

$$A_{3694} = 0.0816[Magnesium] - 0.0139 \quad (17)$$

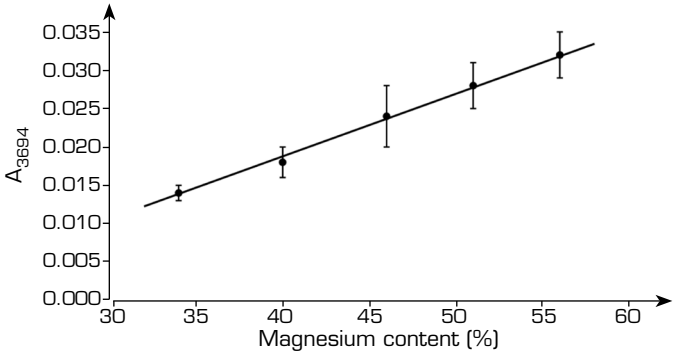

Source: Elaborated by the authors.

Figure 6. Weighted linear regression for magnesium quantification.

Figure 7 illustrates the weighted linear regression of A_{637} versus Teflon content (Eq. 18), employed for the determination of Teflon content. The fit, based on the data from Table 3, yielded a coefficient of determination $R_w^2 = 0.993$.

$$A_{637} = 0.2344[Teflon] - 0.0183 \quad (18)$$

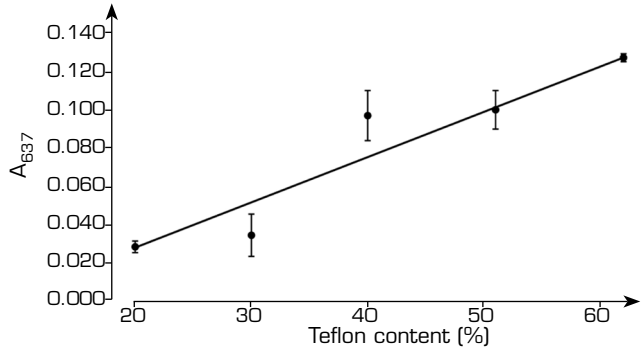

Source: Elaborated by the authors.

Figure 7. Weighted linear regression for Teflon quantification.

For the determination of Viton content, the weighted linear regression of A_{1397} versus Viton content (Eq. 19), with $R_w^2 = 0.942$, is shown in Fig. 8, based on the data from Table 4.

$$A_{1397} = 0.1396[Viton] + 0.0043 \quad (19)$$

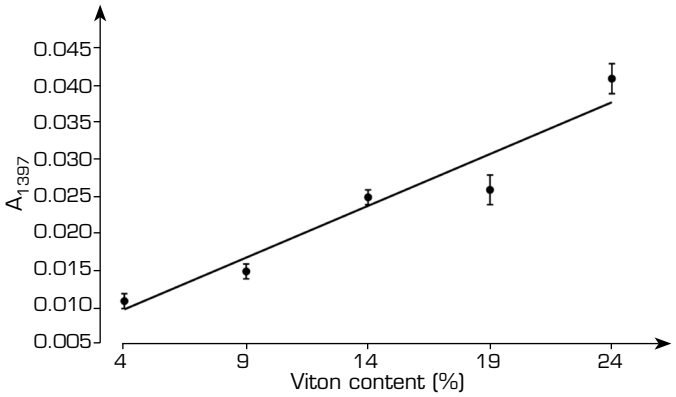

Source: Elaborated by the authors.

Figure 8. Weighted linear regression for Viton quantification.

The median values of the test sample (Table 5) were applied to the system of Eqs. 17–19, yielding the results shown in Table 7.

Table 7. Test sample results obtained by weighted linear regression.

Component	Nominal content (%)	Weighted linear regression	Determined content (%)	Absolute deviation (%)
Magnesium	25	Eq. 17	34.2	+9.2
Teflon	60	Eq. 18	57.3	-2.7
Viton	15	E1. 19	14.8	-0.2

Source: Elaborated by the authors.

The same dataset (Tables 2–4), including the previously discussed relative errors, was used for the weighted linear regressions. Analysis of Table 7 shows that, for magnesium, the concentration estimated using Eq. 17 remained imprecise, with an absolute deviation of +9.2%, despite a high weighted coefficient of determination (R_w^2 = 0.996). For Teflon, the weighted regression (Eq. 18) provided an estimated value of 57.3%, closer to the expected value than the simple regression result (Eq. 15) (56.1%), with R_w^2 = 0.993. In the case of Viton, the weighted regression (Eq. 19) achieved R_w^2 = 0.928, yielding only a minor deviation (-0.2%) with the estimated concentration of 14.8% being close to the nominal value of 15%.

Simple linear regression with CI

For magnesium, using the data from Table 2 in Eq. 9, the following results were obtained:

$$S_{y/x} = 0.00048$$

Using Eq. 14 and A_{3694} = 0.014 (Table 5), the following is obtained:

$$[Magnesium] = x_0 = \frac{0.014 + 0.0148}{0.0836} = 0.344$$

Applying the values in Eq. 10, the following is obtained:

$$S_{x_0} = \frac{0.00048}{0.0836}\sqrt{\frac{1}{5} + \frac{1}{5} + \frac{(0.014 - 0.0232)^2}{0.0836^2 . 0.03034}} = 0.00513$$

At a 95% confidence level with 3 degrees of freedom, $t_{0.95;3} = 3.182$. Using Eq. 11, the estimated CI for the magnesium content is:

$$CI_{Magnésio} = [32.8\% - 36.1\%]$$

For Teflon, the data from Table 3 were applied to Eq. 9, yielding:

$$Sy_{/x} = 0.01564$$

Using Eq. 15 and $A_{637} = 0.116$ (Table 5), the following is obtained:

$$[Teflon] = x_0 = \frac{0.116 + 0.0229}{0.2476} = 0.561$$

Applying the values in Eq. 10, the following is obtained:

$$S_{x_0} = \frac{0.01564}{0.2476}\sqrt{\frac{1}{5} + \frac{1}{5} + \frac{(0.116 - 0.0776)^2}{0.2476^2.\,0.11032}} = 0.04966$$

By substituting into Eq. 11, the estimated CI for Teflon content is ($t_{0.95;3} = 3.182$):

$$CI_{Teflon} = [40.3\% - 71.9\%]$$

For Viton, the data from Table 4 were applied to Eq. 9, yielding:

$$Sy_{/x} = 0.00361$$

Using Eq. 16 and $A_{1397} = 0.025$ (Table 5), the following is obtained:

$$[Viton] = x_0 = \frac{0.025 - 0.0037}{0.1420} = 0.15$$

Applying the values in Eq. 10, the following is obtained:

$$S_{x_0} = \frac{0.00361}{0.1420}\sqrt{\frac{1}{5} + \frac{1}{5} + \frac{(0.025 - 0.0236)^2}{0.1420^2.\,0.025}} = 0.01616$$

By substituting into Eq. 11, with $t_{0.95;3} = 3.182$ the estimated CI for Viton content is:

$$CI_{Viton} = [9.9\% - 20.1\%]$$

Evaluation of results across different linear regression models

Figure 9 shows the results obtained from simple linear regression, weighted linear regression, and linear regression with CIs. For magnesium, the predicted value fell outside the CI, indicating a potential systematic error in the indirect methodology used to determine its content. This deviation may be linked to variations in the test sample affecting the -OH concentration, such as imprecise temperature control during the preparation of samples A1-A5 and the test sample itself. An alternative approach to determining the magnesium content is to calculate the difference from 100% of the combined Viton and Teflon contents. In this

case, the value obtained using simple linear regression is 28.9%, whereas weighted linear regression yields 27.9%, which is closer to the nominal value of 25%. For Teflon and Viton, the estimates from both simple and weighted regressions fell within the CI. Notably, for Teflon, the weighted regression provided an estimate 1.2% closer to the true value, whereas for Viton, both methods yielded nearly identical results (15% versus 14.8%).

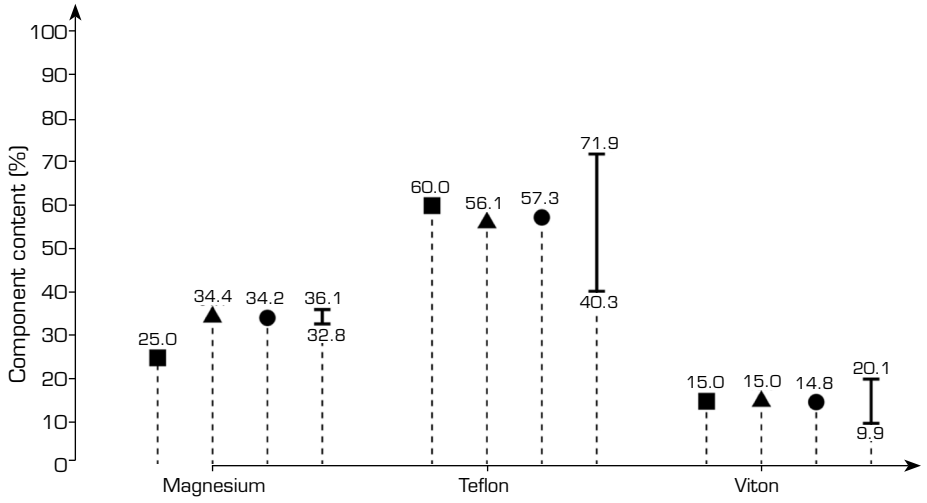

Source: Elaborated by the authors.

Figure 9. Results for the test-sample contents: reference values (■); values obtained using simple linear regression (▲); values obtained using weighted linear regression (●); and simple linear regression with 95%CIs (|).

CONCLUSION

The results of this study demonstrate that the FT-IR/UATR methodology, applied to as-received MTV pyrotechnic compositions, provides an effective approach for analyzing unknown samples, even in the presence of notable sampling errors, while accounting for the specific characteristics of the materials. This work contributes to filling a gap in the scientific literature on the quantification of components in pyrotechnic systems, through the assessment of various statistical models, including one specifically developed for FT-IR spectroscopy.

Moreover, the proposed methodology offers a significant advancement for quality control in the aerospace and defense industries, providing a rapid, accurate, and non-destructive means of analyzing unknown compositions and proving especially valuable for reverse engineering applications.

CONFLICTS OF INTEREST

Nothing to declare.

AUTHOR CONTRIBUTIONS

Conceptualization: Julio BHS and Dutra RCL; **Methodology:** Julio BHS and Diniz MF; **Computational Works:** Julio BHS; **Funding Acquisition:** Dutra RCL; **Analysis:** Julio BHS, Dutra RCL, Cavalcante JA, and Diniz MF; **Writing – Original Draft Preparation:** Julio BHS; **Writing – Review & Editing:** Julio BHS, Cavalcante JA, and Dutra RCL; **Supervision:** Dutra RCL; **Final approval**: Julio BHS.

DATA AVAILABILITY STATEMENT

All data sets were generated or analyzed in the current study.

FUNDING

Coordenação de Aperfeiçoamento de Pessoal de Nível Superior
Finance code 001
Conselho Nacional de Desenvolvimento Científico e Tecnológico
Grant No: 301626/2022-7

DECLARATION OF USEOF ARTIFICIAL INTELLIGENCE TOOLS

Artificial intelligence was not used.

ACKNOWLEDGEMENTS

Not applicable.

REFERENCES

Agrawal JP (2010) High energy materials: propellants, explosives and pyrotechnics. Weinheim: Wiley. https://doi.org/10.1002/9783527628803

Barros AH, Magalhães RF, Murakami LMS, Diniz MF, Sanches NB, Carvalho TA, Dutra JCN, Dutra RCL (2025) Determination of elastomer content in NR/SBR/BR blends. Polímeros 35(2):1-11. https://doi.org/10.1590/0104-1428.20240110

Barros L (2016) Qualificação de composições pirotécnicas usadas no sistema de ignição de motor foguete a propelente sólido (master's thesis). São José dos Campos: Instituto Tecnológico de Aeronáutica. In Portuguese. http://www.bdita.bibl.ita.br/tesesdigitais/71821.pdf

Dozono PT (2003) Avaliação do desempenho de composições pirotécnicas para a ignição de propelentes sólidos (master's thesis). São José dos Campos: Instituto Tecnológico de Aeronáutica. In Portuguese. http://www.bdita.bibl.ita.br/tesesdigitais/000499552.pdf

Draper NR, Smith H (1998) Applied regression analysis. 3rd ed. New York: Wiley. https://doi.org/10.1002/9781118625590

Dutra RCL, Lourenço VL, Diniz MF, Azevedo MFP, Barbosa RV, Soares BG (1996) Poly(ethylene-co-vinyl acetate-co-vinyl mercaptoacetate) (EVALSH): determination of the vinyl mercaptoacetate content by thermogravimetric analysis and FTIR spectroscopy. Polym Bull 36(5):593-600. https://doi.org/10.1007/BF00342451

Dutra RCL, Soares BG (1998) Determination of the vinyl mercaptoacetate content in poly(ethylene-co-vinyl acetate-co-vinyl mercaptoacetate) (EVASH) by TGA analysis and FTIR spectroscopy. Polym Bull 41(1):61-67. https://doi.org/10.1007/s002890050333

Farias SL, Costa LG, Calili RF, Rios RM, Oliveira EC (2015) Avaliação metrológica da curva analítica para determinação do teor de enxofre em baixíssimas concentrações em óleo diesel S10. Quím Nova 38(6):852-858. https://doi.org/10.5935/0100-4042.20150071

Gaunekar S, Ambekar A (2024) Effect of hygrothermal aging on the decomposition reactions of magnesium/Teflon/Viton (MTV) pyrotechnic. Propellants Explos Pyrotech 50(2):1-13. https://doi.org/10.1002/prep.202400162

Horák VM, Vítek A (1978) Interpretation and processing of vibrational spectra. New York: John Wiley and Sons.

Koch EC (2002) Metal-fluorocarbon-pyrolants: III. Development and application of magnesium/Teflon 850A®/Viton® (MTV). Propellants Explos Pyrotech 27(5):262-266. https://doi.org/10.1002/1521-4087(200211)27:5<262::AID-PREP262>3.0.CO;2-8

Koch EC (2012) Metal-fluorocarbon based energetic materials: chemistry of the violent reaction. Weinheim: Wiley-VCH. https://doi.org/10.1002/9783527644186

Mattos EC, Diniz MF, Nakamura NM, Dutra RCL (2009) Determination of polymer content in energetic materials by FT-IR. J Aerosp Technol Manag 1(2):167-175. Available at https://www.scielo.br/j/jatm/a/tXQZdrVyCMfNs3pNbzpsm6Q/?format=pdf&lang=en

Miller JN, Miller JC (2010) Statistics and chemometrics for analytical chemistry. 6th ed. Harlow: Pearson Education Limited.

Montgomery DC, Peck EA, Vining GG (2012) Introduction to linear regression analysis. 5th ed. Hoboken: John Wiley & Sons.

Palmerio AF (2017) Introdução à tecnologia de foguete. 2nd ed. São José dos Campos: SindCT.

Pires HB, Rocha RJ, Iha K, Binda RV, Rocco JAFF (2017) Influência do envelhecimento acelerado em flares magnésio/PTFE/FPM. Quím Nova 40(8):865-870. https://doi.org/10.21577/0100-4042.20170093

Smith AL (1979) Applied infrared spectroscopy. New York: John Wiley & Sons.

Thompson JM (2018) Infrared spectroscopy. New York: Jenny Stanford Publishing. https://doi.org/10.1201/9781351206037-4

Zahir MH, Rahman MM, Irshad K, Rahman MM (2019) Shape-stabilized phase change materials for solar energy storage: MgO and $Mg(OH)_2$ mixed with polyethylene glycol. Nanomaterials 9(12):1-21. https://doi.org/10.3390/nano9121773